Extraction of entanglement from quantum fields with entangled particle detectors

Dyuman Bhattacharya,[1,*] Kensuke Gallock-Yoshimura,[1,†] Laura J. Henderson,[2,1,‡] and Robert B. Mann[1,§]

[1]*Department of Physics and Astronomy, University of Waterloo, Waterloo, Ontario, N2L 3G1, Canada*
[2]*Centre for Engineered Quantum Systems, School of Mathematics and Physics, The University of Queensland, St. Lucia, Queensland 4072, Australia*

(Received 3 January 2023; accepted 13 April 2023; published 11 May 2023)

We consider two initially entangled Unruh-DeWitt particle detectors and examine how the initial entanglement changes after interacting with a quantum scalar field. Just as initially separable detectors can extract entanglement from the field, entangled detectors also can gain more entanglement so long as they are weakly correlated at the beginning. For initially sufficiently entangled detectors, only degradation takes place. We then apply our analysis to a gravitational shock wave spacetime and show that a shock wave can enhance the initial entanglement of weakly entangled detectors. Moreover, we find that this enhancement can occur for greater detector separations than in Minkowski spacetime.

DOI: 10.1103/PhysRevD.107.105008

I. INTRODUCTION

It is well known by now that a vacuum state of a quantum field is an entangled state [1,2]. One can examine such entanglement by making use of a particle detector, which is a nonrelativistic first-quantized system locally coupled to the field. A commonly used model is a two-level quantum system known as an Unruh-DeWitt (UDW) detector [3,4], which is known to capture the essence of light-matter interactions when no angular momentum is exchanged [5–7]. For example, two initially uncorrelated UDW detectors (e.g., both in their ground states) can become entangled after interacting with a quantum scalar field even when they are causally disconnected. In other words, the detectors extract entanglement from the field without directly exchanging quanta. Such a protocol is known as *entanglement harvesting* [8–13], and the amount of harvested entanglement is sensitive to the state of motion of the detectors and the geometry of underlying spacetime [14–22].

One can also think of initially entangled detectors and ask how much their initial entanglement changes as a function of their motion and the structure of spacetime. If their initial entanglement is maximal (e.g., a Bell state) then their entanglement will necessarily decrease since after the interaction the detectors will be correlated with the field, and the monogamy of entanglement tells us that the detectors must lose their initial correlation. In general, the phenomenon of losing initial entanglement is known as *entanglement degradation*. This phenomenon has been known for quite some time for accelerating observers [23–25], with a number of subsequent studies [26–36] carried out for entangled UDW-type detectors.

Entanglement harvesting and degradation suggest that two initially entangled detectors can either gain or lose entanglement after interacting with the field. One then can ask what the conditions are for enhancement and degradation of entanglement. Such a question was considered for two inertial harmonic-oscillator type UDW detectors in Minkowski spacetime [27], in which the time dependence of the initial entanglement was analyzed by using the quantum Langevin equation with an assumption that the detectors interact with the field for an infinitely long time after being suddenly switched on. The initial entanglement was found to decrease with time, vanishing at the end.

Here we instead consider how much the initial entanglement of a pair of UDW detectors changes after interacting with a field for a finite duration of time, working perturbatively in the field coupling. It is known that such a method has a technical difficulty: in a perturbative analysis, the density matrix of entangled pointlike UDW detectors contains divergent elements [32]. One way to circumvent this issue is to use finite-sized detectors. Although one must face tedious calculations in a generic curved spacetime, inertial detectors in Minkowski spacetime are tractable and yet the fate of entanglement in such a simple setting has not been examined. Another route is to apply an approximation to a measure of entanglement [35]: the divergent elements in the density matrix only appear in the higher order terms in the coupling constant. Quantifying the amount of entanglement between the detectors via negativity, we can ignore such a divergent term for sufficiently small

[*]d7bhatta@uwaterloo.ca
[†]kgallock@uwaterloo.ca
[‡]laura.henderson@uq.edu.au
[§]rbmann@uwaterloo.ca

coupling. However, this approximation is valid only for initially sufficiently entangled detectors, and cannot be applied to initially weakly entangled ones.

We investigate in this paper the extraction of vacuum entanglement by two entangled inertial detectors in Minkowski spacetime, considering situations in which the detectors are initially nearly maximally entangled and initially weakly entangled, complementing previous work in this subject [12] for initially separable detectors. Introducing finite-sized UDW detectors to make their density matrix well defined, we employ concurrence as a measure of entanglement. We examine the effects of the divergent terms on this quantity, and provide an approximation that consistently allows us to neglect such terms. We show that these approximations are valid even for pointlike detectors, and utilize them to show that *weakly entangled detectors can extract more entanglement from the field even when they are causally disconnected*.

We then extend our analysis to consider a gravitational shock wave spacetime [20] and explore the effect of a shock wave on the initial entanglement between pointlike detectors. We have chosen the shock wave spacetime since it provides the simplest nontrivial comparison with Minkowski spacetime: the Wightman function is everywhere the same as that in Minkowski spacetime except along the null trajectory of the shock. This allows us to make a clear comparison with the case of entanglement harvesting for initially entangled UDW detectors in pure Minkowski spacetime. We find that a shock wave can enhance entanglement compared to the Minkowski spacetime case: the detectors are able to gain entanglement with smaller energy gaps and larger amounts of initial entanglement.

Our paper is organized as follows. We begin with providing a density matrix of initially entangled detectors after interacting with a quantum scalar field in Sec. II A. The divergence in the density matrix does not show up in the concurrence after performing approximations in Sec. II B. We then examine the fate of initial entanglement in $(3+1)$-dimensional Minkowski (Sec. III) and shock wave spacetimes (Sec. IV), followed by conclusions in Sec. V. We will use natural units, $\hbar = c = 1$, and denote spacetime points by $\mathsf{x} = (t, \boldsymbol{x})$.

II. INITIALLY ENTANGLED DETECTORS

A. Density matrix

We shall consider two UDW detectors A and B, linearly coupled to a quantum scalar field. Let τ_j ($j \in \{\mathrm{A}, \mathrm{B}\}$) be the proper time of detector j and t a common time (i.e., a time parameter that describes both detectors). The interaction Hamiltonian in the interaction picture is given by

$$\hat{H}_{\mathrm{I}}(t) = \frac{\mathrm{d}\tau_{\mathrm{A}}}{\mathrm{d}t}\hat{H}_{\mathrm{A}}(\tau_{\mathrm{A}}(t)) + \frac{\mathrm{d}\tau_{\mathrm{B}}}{\mathrm{d}t}\hat{H}_{\mathrm{B}}(\tau_{\mathrm{B}}(t)), \tag{1}$$

where $\hat{H}_j(\tau_j)$ is

$$\hat{H}_j(\tau_j) = \lambda_j \chi_j(\tau_j)\hat{\mu}_j(\tau_j) \otimes \int \mathrm{d}^3x F_j(\boldsymbol{x}-\boldsymbol{x}_j)\hat{\phi}(\mathsf{x}_j(\tau_j)). \tag{2}$$

Here, λ_j is the coupling constant between detector j and the field $\hat{\phi}$, $\chi_j(\tau_j)$ is a switching function that specifies how a detector interacts, and $\hat{\mu}_j(\tau_j)$ is a monopole moment given by

$$\hat{\mu}_j(\tau_j) \coloneqq e^{\mathrm{i}\Omega_j\tau_j}|e_j\rangle\langle g_j| + e^{-\mathrm{i}\Omega_j\tau_j}|g_j\rangle\langle e_j| \tag{3}$$

with Ω_j being the energy gap between the ground $|g_j\rangle$ and excited $|e_j\rangle$ states. $F_j(\boldsymbol{x}-\boldsymbol{x}_j)$ is the so-called smearing function, which specifies the spatial profile and the center of mass position $\boldsymbol{x}_j$ of detector j. As an example, one can choose the Dirac delta distribution to make the detector pointlike.

The time-evolution operator, $\hat{U}_{\mathrm{I}}$, can be written by using a time-ordering symbol, $\mathcal{T}_t$, with respect to the common time t:

$$\hat{U}_{\mathrm{I}} = \mathcal{T}_t \exp\left(-\mathrm{i}\int_{\mathbb{R}} \mathrm{d}t\, \hat{H}_{\mathrm{I}}(t)\right) \tag{4}$$

$$= \hat{U}_{\mathrm{I}}^{(0)} + \hat{U}_{\mathrm{I}}^{(1)} + \hat{U}_{\mathrm{I}}^{(2)} + \mathcal{O}(\lambda^3), \tag{5}$$

where $\hat{U}_{\mathrm{I}}^{(j)}$ is the jth power of the coupling constant λ:

$$\hat{U}_{\mathrm{I}}^{(0)} \coloneqq \mathbb{1}, \tag{6}$$

$$\hat{U}_{\mathrm{I}}^{(1)} \coloneqq -\mathrm{i}\int_{\mathbb{R}} \mathrm{d}t\, \hat{H}_{\mathrm{I}}(t), \tag{7}$$

$$\hat{U}_{\mathrm{I}}^{(2)} \coloneqq -\int_{\mathbb{R}} \mathrm{d}t_1 \int_{-\infty}^{t_1} \mathrm{d}t_2\, \mathcal{T}_t[\hat{H}_{\mathrm{I}}(t_1)\hat{H}_{\mathrm{I}}(t_2)]. \tag{8}$$

Let us assume that the field is in the vacuum state, $|0\rangle$, and the detectors A and B are initially entangled,

$$|\Psi_0\rangle = (\alpha|g_{\mathrm{A}}\rangle|g_{\mathrm{B}}\rangle + \beta e^{\mathrm{i}\theta}|e_{\mathrm{A}}\rangle|e_{\mathrm{B}}\rangle)|0\rangle, \tag{9}$$

where $\alpha, \beta \in [0,1]$ with $\alpha^2 + \beta^2 = 1$ and $\theta \in [0, 2\pi)$ is the relative phase. For example, $\alpha = 0$, 1 correspond to separable states while $\alpha = 1/\sqrt{2}$ gives a Bell state. We will refer to $\alpha = 1$ as the entanglement harvesting scenario. Unless otherwise stated, we let $\beta = \sqrt{1-\alpha^2}$ throughout this paper. Note that we could also consider initial states of the form

$$|\Psi_0\rangle = (\alpha|g_{\mathrm{A}}\rangle|e_{\mathrm{B}}\rangle + \beta e^{\mathrm{i}\theta}|g_{\mathrm{B}}\rangle|e_{\mathrm{A}}\rangle)|0\rangle, \tag{10}$$

by applying a bit-flip gate $\mathbb{1}_{\mathrm{A}} \otimes \hat{\sigma}_x$ and setting $\Omega_{\mathrm{B}} \to -\Omega_{\mathrm{B}}$; the resultant behavior in this case is qualitatively similar to what we present below, as was the case for an earlier nonperturbative analysis of harvesting of mutual information [34].

One can obtain the state of the detectors, ρ_{AB}, after the interaction by tracing out the field degree of freedom. Writing $\rho_0 \coloneqq |\Psi_0\rangle\langle\Psi_0|$, we obtain

$$\rho_{\mathrm{AB}} = \mathrm{Tr}_\phi[\hat{U}_{\mathrm{I}}\rho_0\hat{U}_{\mathrm{I}}^\dagger] \tag{11}$$

$$\begin{aligned} &= \mathrm{Tr}_\phi[\rho_0] + \mathrm{Tr}_\phi[\hat{U}_{\mathrm{I}}^{(1)}\rho_0\hat{U}_{\mathrm{I}}^{(1)\dagger}] \\ &\quad + \mathrm{Tr}_\phi[\hat{U}_{\mathrm{I}}^{(2)}\rho_0] + \mathrm{Tr}_\phi[\rho_0\hat{U}^{(2)\dagger}] + \mathcal{O}(\lambda^4). \end{aligned} \tag{12}$$

In the basis $\{|g_{\mathrm{A}}g_{\mathrm{B}}\rangle, |g_{\mathrm{A}}e_{\mathrm{B}}\rangle, |e_{\mathrm{A}}g_{\mathrm{B}}\rangle, |e_{\mathrm{A}}e_{\mathrm{B}}\rangle\}$, the density matrix ρ_{AB} can be obtained as follows [32]:

$$\rho_{\mathrm{AB}} = \begin{bmatrix} r_{11} & 0 & 0 & r_{14} \\ 0 & r_{22} & r_{23} & 0 \\ 0 & r_{23}^* & r_{33} & 0 \\ r_{14}^* & 0 & 0 & r_{44} \end{bmatrix} + \mathcal{O}(\lambda^4), \tag{13a}$$

$$\begin{aligned} r_{11} &= \alpha^2 + 2\alpha^2\mathrm{Re}[J_{\mathrm{AA}}^{(-+)} + J_{\mathrm{BB}}^{(-+)}] \\ &\quad + 2\alpha\sqrt{1-\alpha^2}\mathrm{Re}[e^{\mathrm{i}\theta}(J_{\mathrm{AB}}^{(--)} + J_{\mathrm{BA}}^{(--)})] \end{aligned} \tag{13b}$$

$$\begin{aligned} r_{14} &= \alpha\sqrt{1-\alpha^2}e^{-\mathrm{i}\theta}(1 + J_{\mathrm{AA}}^{(-+)} + J_{\mathrm{AA}}^{(+-)*} + J_{\mathrm{BB}}^{(-+)} + J_{\mathrm{BB}}^{(+-)*}) \\ &\quad + \alpha^2(J_{\mathrm{AB}}^{(++)*} + J_{\mathrm{BA}}^{(++)*}) + (1-\alpha^2)(J_{\mathrm{AB}}^{(--)} + J_{\mathrm{BA}}^{(--)}) \end{aligned} \tag{13c}$$

$$\begin{aligned} r_{22} &= (1-\alpha^2)I_{\mathrm{AA}}^{(+-)} + 2\alpha\sqrt{1-\alpha^2}\mathrm{Re}[e^{-\mathrm{i}\theta}I_{\mathrm{AB}}^{(++)}] \\ &\quad + \alpha^2 I_{\mathrm{BB}}^{(-+)} \end{aligned} \tag{13d}$$

$$\begin{aligned} r_{23} &= \alpha\sqrt{1-\alpha^2}e^{\mathrm{i}\theta}I_{\mathrm{AA}}^{(--)} + (1-\alpha^2)I_{\mathrm{BA}}^{(+-)} + \alpha^2 I_{\mathrm{AB}}^{(-+)} \\ &\quad + \alpha\sqrt{1-\alpha^2}e^{-\mathrm{i}\theta}I_{\mathrm{BB}}^{(++)} \end{aligned} \tag{13e}$$

$$\begin{aligned} r_{33} &= \alpha^2 I_{\mathrm{AA}}^{(-+)} + 2\alpha\sqrt{1-\alpha^2}\mathrm{Re}[e^{\mathrm{i}\theta}I_{\mathrm{AB}}^{(--)}] \\ &\quad + (1-\alpha^2)I_{\mathrm{BB}}^{(+-)} \end{aligned} \tag{13f}$$

$$\begin{aligned} r_{44} &= (1-\alpha^2) + 2(1-\alpha^2)\mathrm{Re}[J_{\mathrm{AA}}^{(+-)} + J_{\mathrm{BB}}^{(+-)}] \\ &\quad + 2\alpha\sqrt{1-\alpha^2}\mathrm{Re}[e^{-\mathrm{i}\theta}(J_{\mathrm{AB}}^{(++)} + J_{\mathrm{BA}}^{(++)})], \end{aligned} \tag{13g}$$

where

$$\begin{aligned} I_{jk}^{(pq)} &\coloneqq \lambda_j\lambda_k \int_{\mathbb{R}} \mathrm{d}\tau_j \int_{\mathbb{R}} \mathrm{d}\tau_k \chi_j(\tau_j)\chi_k(\tau_k) \\ &\quad \times e^{\mathrm{i}(p\Omega_j\tau_j + q\Omega_k\tau_k)}\mathcal{W}(\mathsf{x}_j(\tau_j), \mathsf{y}_k(\tau_k)), \end{aligned} \tag{14}$$

$$\begin{aligned} J_{jk}^{(pq)} &\coloneqq -\lambda_j\lambda_k \int_{\mathbb{R}} \mathrm{d}\tau_j \int_{-\infty}^{t_1(\tau_j)} \mathrm{d}\tau_k \chi_j(\tau_j)\chi_k(\tau_k) \\ &\quad \times e^{\mathrm{i}(p\Omega_j\tau_j + q\Omega_k\tau_k)}\mathcal{W}(\mathsf{x}_j(\tau_j), \mathsf{y}_k(\tau_k)), \end{aligned} \tag{15}$$

and we have used the fact that $I_{\mathrm{AB}}^{(\pm\pm)} = I_{\mathrm{BA}}^{(\mp\mp)*} \in \mathbb{C}$ in r_{22} and r_{33}, respectively. The elements $I_{\mathrm{AB}}^{(\pm\pm)}$ and $J_{kk}^{(\pm\mp)}$ appear in the density matrix (13a) only for initially entangled detectors.

The quantity

$$\mathcal{W}(\mathsf{x}_j, \mathsf{y}_k) \coloneqq \int \mathrm{d}^3x \int \mathrm{d}^3y\, F_j(\boldsymbol{x}-\boldsymbol{x}_j)F_k(\boldsymbol{y}-\boldsymbol{y}_j)W(\mathsf{x}, \mathsf{y}), \tag{16}$$

where $W(\mathsf{x}, \mathsf{y}) \coloneqq \langle 0|\hat{\phi}(\mathsf{x})\hat{\phi}(\mathsf{y})|0\rangle$ is the Wightman function (two-point vacuum correlation function). In the above equations, the Wightman functions, $W(\mathsf{x}_j(\tau_j), \mathsf{y}_k(\tau_k))$, are pulled back along the trajectories of detectors j and k.

B. Entanglement measure

To quantify the entanglement between the detectors we use the *concurrence*, $\mathcal{C}_{\mathrm{AB}}$. For density matrices of the form (13a), it is known that the qubits are entangled if and only if one of the following is satisfied [14]:

$$|r_{14}|^2 > r_{22}r_{33}, \qquad |r_{23}|^2 > r_{11}r_{44}. \tag{17}$$

We find that $|r_{23}|^2 > r_{11}r_{44}$ can never be realized; thereby the concurrence is defined as

$$\mathcal{C}_{\mathrm{AB}} \coloneqq 2\max\{0, |r_{14}| - \sqrt{r_{22}r_{33}}\}. \tag{18}$$

Note that $0 \leq \mathcal{C}_{\mathrm{AB}} \leq 1$ and $\mathcal{C}_{\mathrm{AB}} = 0$ if and only if two detectors are not entangled. One can easily verify that the initial entanglement in (10) is

$$\mathcal{C}_{\mathrm{AB},0} \coloneqq 2\alpha\sqrt{1-\alpha^2}\left(=2\beta\sqrt{1-\beta^2}\right). \tag{19}$$

Although evaluating the concurrence (18) may seem straightforward, inspection of (13c), (13d), and (13f) indicates that care must be taken in perturbatively approximating $\mathcal{C}_{\mathrm{AB}}$. This is because each of r_{22} and r_{33} are of order λ^2 (and so their geometric mean $\sqrt{r_{22}r_{33}}$ is of order λ^2) whereas a perturbative expansion of r_{14}

$$r_{14} = r_{14}^{(0)} + \lambda^2 r_{14}^{(2)} + \lambda^4 r_{14}^{(4)} + \mathcal{O}(\lambda^6), \tag{20}$$

yields

$$\begin{aligned} |r_{14}|^2 &= |r_{14}^{(0)}|^2 + \lambda^2 2\mathrm{Re}[r_{14}^{(0)}r_{14}^{(2)*}] \\ &\quad + \lambda^4(|r_{14}^{(2)}|^2 + 2\mathrm{Re}[r_{14}^{(0)}r_{14}^{(4)*}]) + \mathcal{O}(\lambda^6). \end{aligned} \tag{21}$$

For initially separable states, (i.e., the standard harvesting protocol) $r_{14}^{(0)} = 0$, and so $|r_{14}|^2 = \lambda^4 |r_{14}^{(2)}|^2 + \mathcal{O}(\lambda^6)$, indicating that there are values of α, close to 0 and 1, for which λ^4 terms must make a significant contribution to $|r_{14}|$. In order to keep the perturbative expansion of $|r_{14}|$ consistent, we will consider cases where the detectors are nearly separable and the case where the detectors are sufficiently entangled separately.

Another issue has to do with the structure of r_{14}, which from (13c) can be written as

$$r_{14}^{(0)} = \alpha\sqrt{1-\alpha^2}e^{-\mathrm{i}\theta}, \tag{22}$$

$$\lambda^2 r_{14}^{(2)} = \lambda^2\Big[\alpha\sqrt{1-\alpha^2}e^{-\mathrm{i}\theta}(Y_\mathrm{A}+Y_\mathrm{B}) + \alpha^2 X_\mathrm{AB}^*(-\Omega) + (1-\alpha^2)X_\mathrm{AB}(\Omega)\Big], \tag{23}$$

where

$$\lambda^2 Y_k \equiv J_{kk}^{(-+)} + J_{kk}^{(+-)*}, \tag{24a}$$

$$\lambda^2 X_\mathrm{AB}(\Omega) \equiv J_\mathrm{AB}^{(--)} + J_\mathrm{BA}^{(--)}, \tag{24b}$$

$$\lambda^2 X_\mathrm{AB}^*(-\Omega) \equiv J_\mathrm{AB}^{(++)*} + J_\mathrm{BA}^{(++)*}. \tag{24c}$$

The imaginary part of Y_k is divergent and causes problems in the pointlike limit [32]. Although it can be regularized by introducing a smearing function, we shall demonstrate that it does not appear in the concurrence under the approximations we consider.

C. Approximating the concurrence

We consider three scenarios: (i) initial weak entanglement with $\alpha \approx 0$; (ii) initial weak entanglement with $\alpha \approx 1$; and (iii) initial sufficient entanglement.

1. Initial weak entanglement: $\alpha \approx 0$

Let us assume that $\alpha \ll 1$ and perform a series expansion of Eq. (21) in terms of $\lambda^n \alpha^m$:

$$|r_{14}|^2 = \underbrace{\alpha^2(1-\alpha^2)}_{\text{initial}} + \underbrace{2\lambda^2\alpha\mathrm{Re}[X_\mathrm{AB}(\Omega)e^{\mathrm{i}\theta}]}_{\text{neutral}} + \underbrace{\lambda^4|X_\mathrm{AB}(\Omega)|^2}_{\text{harvesting}} + \underbrace{2\lambda^2\alpha^2\mathrm{Re}[Y_\mathrm{A}+Y_\mathrm{B}]}_{\text{degradation}} + \mathcal{O}(\lambda^n\alpha^m). \quad (n+m>4). \tag{25}$$

As one can see, $r_{14}^{(4)}$ and the divergent element $\mathrm{Im}[Y_k]$ do not exist in the lower-order terms.

2. Initial weak entanglement: $\alpha \approx 1$

In the same manner, one can obtain a similar expression for $\alpha \approx 1$. For simplicity, let us use $\beta = \sqrt{1-\alpha^2}$ and expand Eq. (21) around $\beta = 0$:

$$|r_{14}|^2 = \underbrace{\beta^2(1-\beta^2)}_{\text{initial}} + \underbrace{2\lambda^2\beta\mathrm{Re}[X_\mathrm{AB}^*(-\Omega)e^{\mathrm{i}\theta}]}_{\text{neutral}} + \underbrace{\lambda^4|X_\mathrm{AB}(-\Omega)|^2}_{\text{harvesting}} + \underbrace{2\lambda^2\beta^2\mathrm{Re}[Y_\mathrm{A}+Y_\mathrm{B}]}_{\text{degradation}} + \mathcal{O}(\lambda^n\beta^m). \quad (n+m>4). \tag{26}$$

As before, the elements $r_{14}^{(4)}$ and $\mathrm{Im}[Y_k]$ are absent. Note that $\beta = 0$ reduces to the entanglement harvesting scenario: $|r_{14}| = \lambda^2|X_\mathrm{AB}(-\Omega)|$.

In both cases $\alpha \approx 0$ and 1, the approximated $|r_{14}|^2$ consists of four parts. The initial entanglement contribution is $\alpha^2(1-\alpha^2)$ in (25) [equivalent to $\beta^2(1-\beta^2)$ in (26)]. The third term containing $X_\mathrm{AB}(\Omega)$ is the part contributing to entanglement harvesting, and so will enhance entanglement. The last term, containing $\mathrm{Re}[Y_\mathrm{A}+Y_\mathrm{B}]$, depends only on each detector and not on their correlations. This term corresponds to an outcome of local operations and so never enhances entanglement. Indeed, one can straightforwardly show that $\lambda^2\mathrm{Re}[Y_j] = -(I_{jj}^{(-+)} + I_{jj}^{(+-)})/2 \le 0$ and so degrades entanglement. The second term, which we denote as the neutral contribution, can be either positive or negative. By choosing the relative phase θ appropriately, we can ensure that $\mathrm{Re}[e^{\mathrm{i}\theta}X_\mathrm{AB}] > 0$, which enhances entanglement.

In summary, we see from (18) that the detectors gain entanglement after the interaction provided the harvesting part is greater than the other two parts in $|r_{14}|$ and $\sqrt{r_{22}r_{33}}$. Indeed, if the harvesting part does not exceed *both* the initial and degradation contributions to $|r_{14}|$, then entanglement degradation is inevitable, regardless of the value of $\sqrt{r_{22}r_{33}}$ since this term *always* contributes to entanglement degradation as it is positive and is subtracted from $|r_{14}|$. This is not the case for harvesting: even if the harvesting contribution is greater than the other two in $|r_{14}|$, entanglement enhancement is not ensured because this depends on $\sqrt{r_{22}r_{33}}$.

3. Initial sufficient entanglement

In this approximation we assume $|r_{14}^{(0)}|^2 \gg \mathcal{O}(\lambda^4)$ and write Eq. (21) explicitly as [35]

$$|r_{14}^{(0)}|^2 = \alpha^2(1-\alpha^2), \tag{27a}$$

$$\mathrm{Re}[r_{14}^{(0)}r_{14}^{(2)*}] = \alpha\sqrt{1-\alpha^2}\Big[\alpha\sqrt{1-\alpha^2}\mathrm{Re}[Y_\mathrm{A}+Y_\mathrm{B}] + \Big(\alpha^2\mathrm{Re}[X_\mathrm{AB}^*(-\Omega)e^{\mathrm{i}\theta}] + (1-\alpha^2)\mathrm{Re}[X_\mathrm{AB}(\Omega)e^{\mathrm{i}\theta}]\Big)\Big], \tag{27b}$$

$$
\begin{aligned}
|r_{14}^{(2)}|^2 = &|\alpha^2 X_{\mathrm{AB}}^*(-\Omega) + (1-\alpha^2) X_{\mathrm{AB}}(\Omega)|^2 \\
&+ \alpha^2(1-\alpha^2)|Y_{\mathrm{A}} + Y_{\mathrm{B}}|^2 \\
&+ 2\alpha\sqrt{1-\alpha^2}\Big(\alpha^2 \mathrm{Re}[X_{\mathrm{AB}}^*(-\Omega)(Y_{\mathrm{A}}+Y_{\mathrm{B}})^* e^{\mathrm{i}\theta}] \\
&+ (1-\alpha^2)\mathrm{Re}[X_{\mathrm{AB}}(\Omega)(Y_{\mathrm{A}}+Y_{\mathrm{B}})^* e^{\mathrm{i}\theta}]\Big). \qquad (27c)
\end{aligned}
$$

Omitting the λ^4 terms, we obtain

$$
|r_{14}|^2 \approx |r_{14}^{(0)}|^2 + \lambda^2 2\mathrm{Re}[r_{14}^{(0)} r_{14}^{(2)*}] \qquad (28)
$$

which is also independent of $r_{14}^{(4)}$ and $\mathrm{Im}[Y_k]$. Obviously this approximation does not work for $\alpha = 0$ and 1 since it cannot recover the entanglement harvesting results. In fact, as in the previous approximations, Eq. (28) consists of three components: the initial entanglement, the harvesting contribution, and the degradation contribution. However now the harvesting contribution does not contain $|X_{\mathrm{AB}}(\Omega)|^2$ or $|X_{\mathrm{AB}}^*(-\Omega)|^2$. Note that for $\alpha \ll 1$ the leading term in (27c) yields the harvesting contribution in (25) [and likewise for $\beta \ll 1$ the harvesting contribution in (26) is recovered].

Henceforth we shall consider these approximations (which are applicable even to pointlike detectors) in evaluating the concurrence in the scenarios we consider.

D. Smeared detectors in a flat spacetime

We now compute the elements in the density matrix (13a) in $(3+1)$-dimensional Minkowski spacetime. We assume that the detectors are identical (have the same shape and internal structure) and are both at rest in a single frame of reference. We choose the switching function, $\chi_j(\tau_j)$, and smearing function, $F_j(\boldsymbol{x}-\boldsymbol{x}_j)$, to be Gaussian functions:

$$
\chi_j(\tau_j) = e^{-(\tau_j - \tau_{j,0})^2/T^2}, \qquad (29)
$$

$$
F_j(\boldsymbol{x}-\boldsymbol{x}_j) = \frac{1}{(\sqrt{\pi}\sigma)^3} e^{-(\boldsymbol{x}-\boldsymbol{x}_j)^2/\sigma^2}, \qquad (30)
$$

where $\tau_{j,0}$ and $\boldsymbol{x}_j$ are their respective centers and T and σ are their respective temporal and spatial widths.

As we show in the Appendix, the quantities $J_{kk}^{(-+)} + J_{kk}^{(+-)*}$, $J_{\mathrm{AB}}^{(++)*}$, and $J_{\mathrm{AB}}^{(--)}$ in r_{14}, and $I_{jk}^{(\pm\pm)}$ in r_{22} and r_{33} are then given by

$$
\begin{aligned}
\lambda_k^2 Y_k \equiv& J_{kk}^{(-+)} + J_{kk}^{(+-)*} \\
=& -\frac{\lambda_k^2 e^{-T^2\Omega^2/2}}{8\pi(1+\sigma^2/T^2)^{3/2}}\left[2\sqrt{1+\sigma^2/T^2} + e^{T^2\Omega^2/2(1+\sigma^2/T^2)}\sqrt{2\pi}T\Omega\,\mathrm{erf}\left(\frac{T\Omega}{\sqrt{2(1+\sigma^2/T^2)}}\right)\right] \\
&- \mathrm{i}\frac{\lambda_k^2 T^2}{8\pi}\int_0^\infty \mathrm{d}|\boldsymbol{k}||\boldsymbol{k}|e^{-|\boldsymbol{k}|^2\sigma^2/2}\left[e^{-T^2(|\boldsymbol{k}|-\Omega)^2/2}\mathrm{erfi}\left(\frac{T(|\boldsymbol{k}|-\Omega)}{\sqrt{2}}\right) - e^{-T^2(|\boldsymbol{k}|+\Omega)^2/2}\mathrm{erfi}\left(\frac{T(|\boldsymbol{k}|+\Omega)}{\sqrt{2}}\right)\right], \qquad (31a)
\end{aligned}
$$

$$
J_{\mathrm{AB}}^{(--)} = -\frac{\lambda_{\mathrm{A}}\lambda_{\mathrm{B}}T^2}{8\pi L} e^{-\mathrm{i}\Omega(t_{\mathrm{A},0}+t_{\mathrm{B},0})} e^{-T^2\Omega^2/2}\int_0^\infty \mathrm{d}|\boldsymbol{k}| e^{-|\boldsymbol{k}|^2(\sigma^2+T^2)/2} e^{\mathrm{i}\Delta t|\boldsymbol{k}|}\mathrm{erfc}\left(\frac{\Delta t + \mathrm{i}T^2|\boldsymbol{k}|}{\sqrt{2}T}\right)\sin(|\boldsymbol{k}|L), \qquad (31b)
$$

$$
I_{kk}^{(-+)} = \frac{\lambda_k^2 e^{-T^2\Omega^2/2}}{8\pi(1+\sigma^2/T^2)^{3/2}}\left[2\sqrt{1+\sigma^2/T^2} - \sqrt{2\pi}T\Omega e^{T^2\Omega^2/2(1+\sigma^2/T^2)}\mathrm{erfc}\left(\frac{T\Omega}{\sqrt{2(1+\sigma^2/T^2)}}\right)\right], \qquad (31c)
$$

$$
I_{\mathrm{AB}}^{(++)} = \frac{\mathrm{i}\lambda_{\mathrm{A}}\lambda_{\mathrm{B}} T e^{\mathrm{i}\Omega(t_{\mathrm{A},0}+t_{\mathrm{B},0})} e^{-T^2\Omega^2/2}}{8\pi L\sqrt{1+\sigma^2/T^2}}\sqrt{\frac{\pi}{2}}[e^{-\Gamma_-^2}\mathrm{erfc}(\mathrm{i}\Gamma_-) - e^{-\Gamma_+^2}\mathrm{erfc}(-\mathrm{i}\Gamma_+)], \qquad (31d)
$$

where $L \coloneqq |\boldsymbol{x}_{\mathrm{B}} - \boldsymbol{x}_{\mathrm{A}}|$ and $\Delta t \coloneqq t_{\mathrm{B},0} - t_{\mathrm{A},0}$ are spatial and temporal separation of the detectors' Gaussian peaks [see Fig. 1(a)], and

$$
\Gamma_\pm \coloneqq \frac{L \pm \Delta t}{T\sqrt{2(1+\sigma^2/T^2)}}. \qquad (32)
$$

We remark that $J_{\mathrm{AB}}^{(++)*}$ can be obtained from $J_{\mathrm{AB}}^{(--)}$ by $\Omega \to -\Omega$ and then taking a complex conjugate. In the same manner, one finds $I_{\mathrm{BA}}^{(--)} = I_{\mathrm{AB}}^{(++)*}$. Note that the real part of (31a) is always nonpositive, which means that $\mathrm{Re}[Y_{\mathrm{A}} + Y_{\mathrm{B}}]$ in $|r_{14}|$ acts as noise that inhibits the detectors from gaining entanglement. In fact, in units of Ω, one can verify from (31a) that $\mathrm{Re}[Y_k] \sim -T\Omega$ when $T\Omega \gg 1$ for $\sigma \geq 0$. This suggests that the longer the interaction, the greater the leakage of entanglement, and thereby entanglement extraction becomes more difficult as the interaction duration increases.

Thanks to the smearing function, all the elements in the density matrix are finite and well defined. One can then perform the approximations in Sec. II B and take a limit $\sigma \to 0$ if pointlike detectors are chosen. In the following sections, we will adopt pointlike detectors. The qualitative behavior for smeared detectors is not so different from the pointlike ones. If we were to first take the limit of $\sigma \to 0$ and then perform the approximations employed in Sec. II B the density matrix would be ill defined due to the presence of divergent matrix elements. Note that realistically, all UDW detectors will have some finite size. However, we can consider σ to be smaller than all other relevant length scales in the system, without taking the $\sigma \to 0$ limit.

III. THE FATE OF ENTANGLEMENT BETWEEN INERTIAL DETECTORS

In this section, we consider pointlike ($\sigma \to 0$) detectors in $(3+1)$-dimensional Minkowski spacetime and see how the initial entanglement changes after the interaction.

As shown in Fig. 1(a), suppose the center of mass of detector A is located at the origin and the peak of Gaussian switching is at $t = 0$, with the position of detector B in a spacetime, $(t_{\mathrm{B},0}, \boldsymbol{x}_{\mathrm{B}})$ fixed but variable. In $(3+1)$-dimensional Minkowski spacetime, the detectors can potentially communicate when they are lightlike separated. This is depicted as an orange strip in the figure; detector A can send quanta to detector B once the support of detector B has overlap with this region.

We first ask if initially entangled detectors can gain more entanglement after interacting with their local fields. The answer is *yes*, though we find that the condition is very limited; only initially weakly entangled detectors can gain entanglement.

Consider weakly entangled detectors with $\beta \approx 0$ (i.e., $\alpha \approx 1$). Using (26) to calculate the concurrence $\mathcal{C}_{\mathrm{AB}}$ after the interaction, we illustrate in Fig. 1(b) the difference between the initial and final concurrences of the detectors for $\beta = 10^{-15}$, $\lambda = 1/10$, $\Omega T = 5$, $\sigma/T = 0$, and $\theta = 0$. In particular, we take $\max\{0, \mathcal{C}_{\mathrm{AB}} - \mathcal{C}_{\mathrm{AB},0}\}$ so that we can see the region of entanglement enhancement. We depict with green dots values of the concurrence that are less than its initial value $\mathcal{C}_{\mathrm{AB},0}$ after the interaction. We first note that communication between the detectors greatly assists entanglement extraction, as one can see from Fig. 1(b) that two detectors gain entanglement when they are in causal contact (within the dashed lines). This phenomenon can be explained from the entanglement harvesting viewpoint: communication enhances the value of $|X_{\mathrm{AB}}(-\Omega)|$ in the entanglement harvesting scenario ($\beta = 0$) [37], and this also happens in $|r_{14}|$ in (26). Nevertheless, as described in the previous section, the degradation term $\mathrm{Re}[Y_{\mathrm{A}} + Y_{\mathrm{B}}]$ will suppress this communication assistance if the interaction duration is too long.

One can also ask if noncommunicating detectors can gain entanglement from the field. The answer is also *yes*.

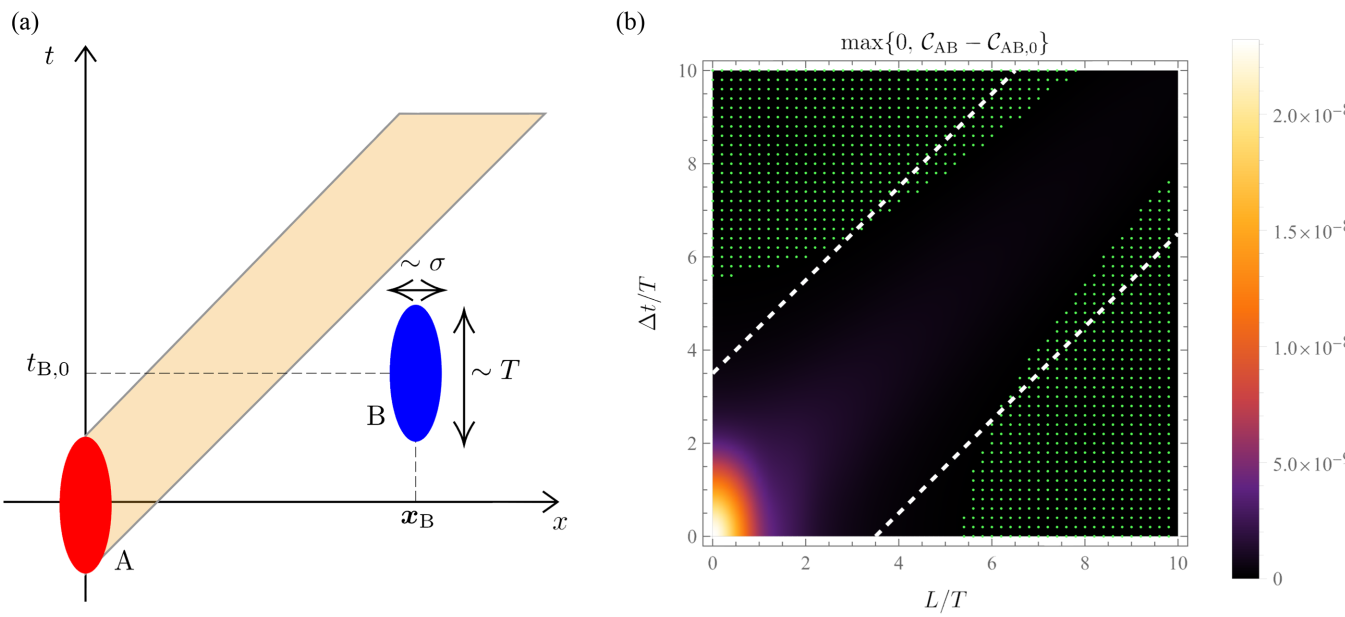

FIG. 1. (a) Finite-sized detectors in Minkowski spacetime. The center of mass of detector B is located at $(t_{\mathrm{B},0}, \boldsymbol{x}_{\mathrm{B}})$; each detector has the respective spatial and temporal Gaussian widths σ and T. The diagonal orange-shaded strip represents the null trajectories from detector A; detector A can directly signal to B by exchanging field quanta once the support of detector B crosses this region. (b) A plot of the positive part of difference $\mathcal{C}_{\mathrm{AB}} - \mathcal{C}_{\mathrm{AB},0}$ between the concurrence before and after the interaction, with $\beta = 10^{-15}$, $\lambda = 1/10$, $\Omega T = 5$, $\sigma/T = 0$, and $\theta = 0$. The green dots represent $\mathcal{C}_{\mathrm{AB}} - \mathcal{C}_{\mathrm{AB},0} \leq 0$, which means the initial entanglement is degraded, and the dashed lines indicate the null trajectory corresponding to the one in (a).

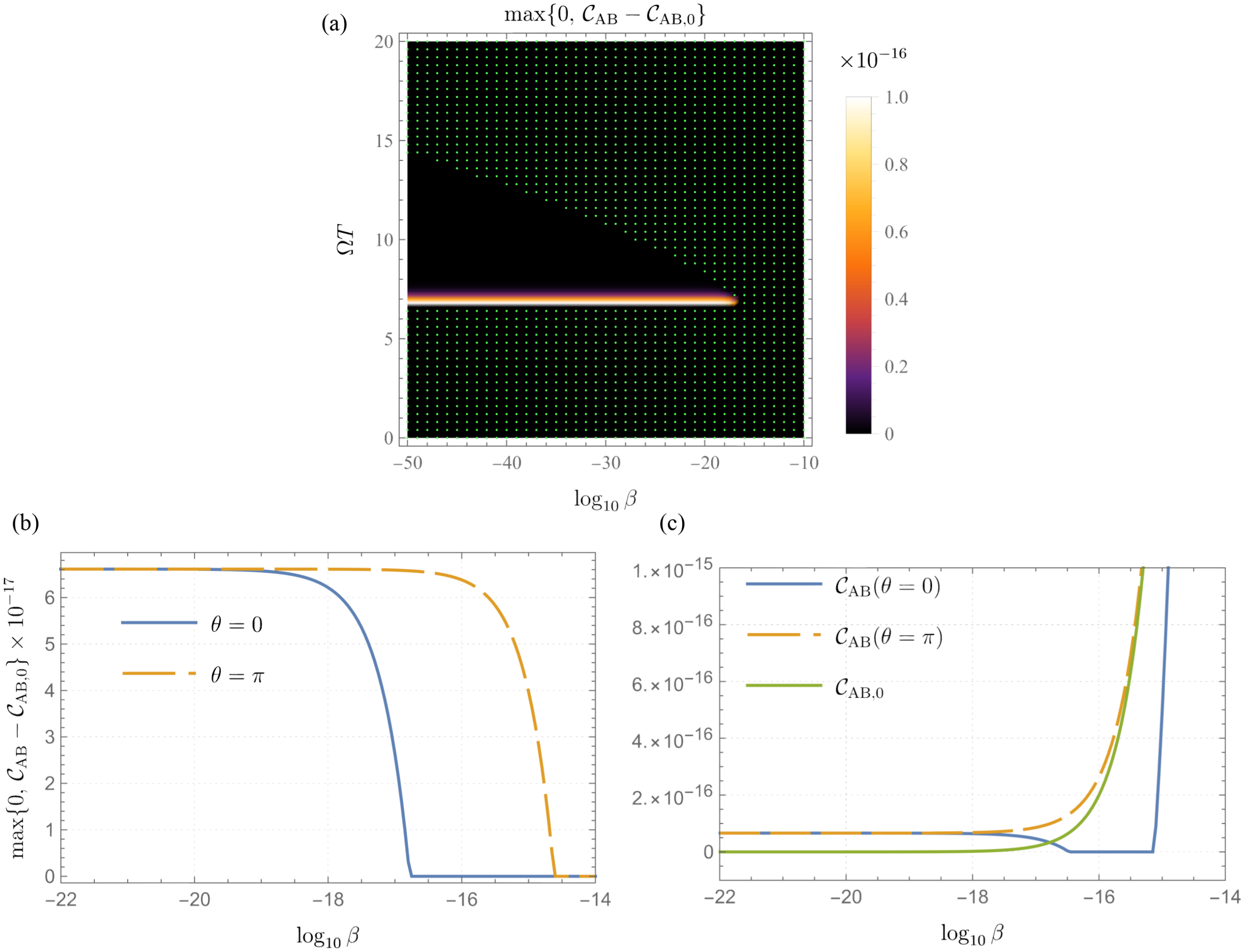

FIG. 2. (a) The positive part of $\mathcal{C}_{\mathrm{AB}} - \mathcal{C}_{\mathrm{AB},0}$ as a function of ΩT and $\log_{10}\beta$ when $\lambda = 1/10$, $L/T = 7$, $\Delta t/T = 0$, $\sigma/T = 0$, and $\theta = 0$. The green dots represent degradation. The detectors can gain entanglement when β is small enough. The range of ΩT that enables the detectors to gain entanglement enlarges as $\beta \to 0$. (b) $\max\{0, \mathcal{C}_{\mathrm{AB}} - \mathcal{C}_{\mathrm{AB},0}\}$ as a function of $\log_{10}\beta$ for $\lambda = 1/10, L/T = 7, \Delta t/T = 0, \sigma/T = 0$, and $\Omega T = 7$. The blue curve shows a slice in (a) at $\Omega T = 7$, whereas the orange dashed curve represents the case when $\theta = \pi$. (c) Each component $\mathcal{C}_{\mathrm{AB}}$ and $\mathcal{C}_{\mathrm{AB},0}$ in (b) with the same parameters.

To see this, we plot concurrence for pointlike detectors ($\sigma/T = 0$) when they are effectively[1] causally disconnected ($L/T = 7$, $\Delta t/T = 0$) in Fig. 2. Figure 2(a) shows the values of ΩT and $\log_{10}\beta$ that enhance entanglement without communication. The parameters are set to be $\lambda = 1/10$, $L/T = 7$, $\Delta t/T = 0$, $\sigma/T = 0$, and $\theta = 0$. Again, the detectors experience degradation when $(\Omega T, \log_{10}\beta)$ is chosen to be a point in the green dots in Fig. 2(a). We find that a pair of causally disconnected detectors can enhance their initial entanglement as long as they are weakly entangled at the beginning. In addition, one must choose ΩT from a suitable range: if the initial entanglement is, for example, $\log_{10}\beta = -30$ with the given parameters, then the energy gap must be $\Omega T \in [6.8, 11]$ to gain more correlation. This energy gap range increases as $\beta \to 0$, namely, the upper bound of Ω to extract entanglement gets pushed to infinity in the limit $\beta \to 0$. We also note that there is a maximum value of β for fixed L/T beyond which entanglement cannot be extracted for any ΩT.

The blue curve in Fig. 2(b) represents a slice at $\Omega T = 7$ in (a), and each factor $\mathcal{C}_{\mathrm{AB}}$ and $\mathcal{C}_{\mathrm{AB},0}$ in $\max\{0, \mathcal{C}_{\mathrm{AB}} - \mathcal{C}_{\mathrm{AB},0}\}$ is shown in 2(c) as blue and green curves, respectively. It is interesting to note from 2(c) that for sufficiently large β, entanglement is completely extinguished after the interaction. There is also a dependence on the relative initial

[1] Since we are using a Gaussian switching, the interaction is not compactly supported in the spacetime. In other words, the detectors are always communicating. However, due to a Gaussian function's exponential suppression, it can be thought of as an effectively compactly supported interaction in $\tau \in [-3.5T + \tau_{j,0}, 3.5T + \tau_{j,0}]$, where τ is a proper time and $\tau_{j,0}$ is the center of Gaussian of detector j [37].

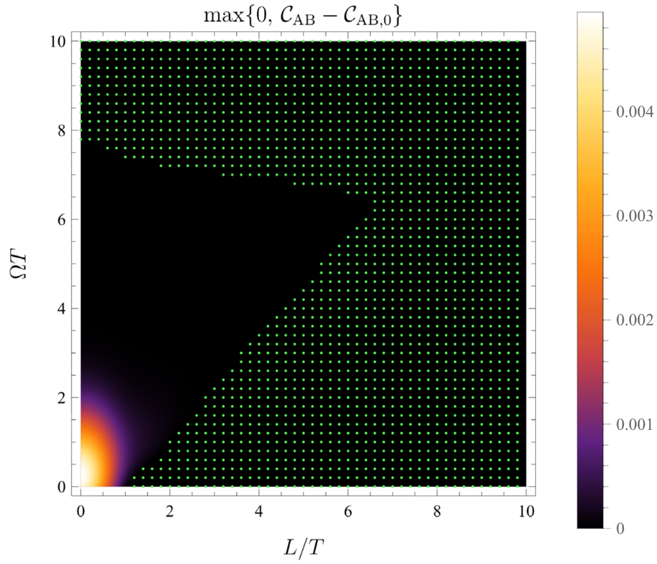

FIG. 3. The positive part of difference $\mathcal{C}_{\rm AB}-\mathcal{C}_{\rm AB,0}$ as a function of L/T and ΩT. Here, $\Delta t/T=0$, $\beta=10^{-15}$, and $\theta=0$. Entanglement degradation occurs in the region with green dots.

phase θ; for $\theta=\pi$ [the orange curve in 2(b) and 2(c)], the positive difference $\mathcal{C}_{\rm AB}-\mathcal{C}_{\rm AB,0}$ persists for larger values of β, allowing for a wider range of entanglement extraction. This dependence on the relative phase θ arises from the term $\mathrm{Re}[X^*_{\rm AB}(-\Omega)e^{-\mathrm{i}\theta}]$ in (26) and elements in $r_{22}r_{33}$.

For the case of initially sufficiently entangled detectors, no entanglement extraction can occur—only degradation takes place. One of the reasons comes from the fact that the degradation part $\mathrm{Re}[Y_{\rm A}+Y_{\rm B}]$ is no longer suppressed in (26) as β grows. Extracting entanglement with $\alpha\approx 0$ is also difficult since $I^{(+-)}_{kk}$ in $\sqrt{r_{22}r_{33}}$ dominates with large Ω.

One notable difference from entanglement harvesting ($\beta=0$) is the energy gap dependence. In the harvesting scenario, detectors with Gaussian switching[2] can extract entanglement even when they are far apart ($L/T\gg 1$) if Ω is large enough [12]. That is, once the detector separation L is fixed, there exists a minimum energy gap $\Omega_{\rm min}$ such that the detectors can harvest entanglement for all $\Omega\geq\Omega_{\rm min}$. In our case, however, this is no longer true. Figure 3 shows $\max\{0,\mathcal{C}_{\rm AB}-\mathcal{C}_{\rm AB,0}\}$ as a function of L/T and ΩT for pointlike detectors with $\Delta t=0$, $\beta=10^{-15}$, and $\theta=0$. That is, we are exploring the region of entanglement extraction in the $(L/T,\Omega T)$ plane when the centers of Gaussian switching in Fig. 1(a) are on the same time slice. We see that there exist minimum and maximum values of Ω for some L that allow detectors to extract entanglement; once Ω gets large enough, only degradation takes place. This is due to a competition between the harvesting part and the degradation part of $|r_{14}|$. When Ω is sufficiently large, the latter quantity is larger than the former, ensuring entanglement degradation. This leads to a maximal value of Ω for which entanglement harvesting is possible. There is also a minimum value of Ω below which harvesting is not possible due to "detector noise"—the positive $\sqrt{r_{22}r_{33}}$ term will be larger than the $|r_{14}|$ term since excitation probabilities increase as the energy gap decreases. The maximum energy gap $\Omega_{\rm max}$ allowing harvesting is pushed to infinity as $\beta\to 0$, recovering the usual harvesting scenario [12].

[2]This is not the case for sudden switching [12].

IV. ENTANGLEMENT IN THE PRESENCE OF A SHOCK WAVE

We now extend our results in Minkowski spacetime to a nontrivial spacetime. We consider in particular a gravitational shock wave spacetime, since it has been shown that a weak gravitational field can enhance entanglement harvesting from the vacuum [38]. Furthermore, for the type of gravitational shock wave that we consider in this paper, the Wightman function for a massless scalar field has a nontrivial, but closed form expression [20].

This latter study considered initially separable detectors in their ground states; we consider here initially entangled detectors with the aim of understanding if the shock wave mitigates or enhances entanglement degradation. We find that a shock wave admits for greater entanglement harvesting relative to the flat space setting, and extends the region in Fig. 2(a) dramatically.

A. Shock wave spacetime

As in [20] we shall be working with the Dray and 't Hooft generalization [39] of the Aichelburg-Sexl shock wave spacetime [40]. Consider a planar shock wave propagating in the z direction in D-dimensional Minkowski spacetime. The metric describing such a spacetime in the so-called Brinkmann coordinates [41] is

$$\mathrm{d}s^2=-\mathrm{d}u\mathrm{d}v+f(\vec{x})\delta(u-u_0)\mathrm{d}u^2+\delta_{ij}\mathrm{d}x^i\mathrm{d}x^j, \qquad (33)$$

where $u=t-z$ and $v=t+z$ are null coordinates, and $\vec{x}$ or x^i, $i\in\{1,\ldots,D-2\}$ are the transverse coordinates (i.e., the remaining spatial coordinates). The wavefront of the shock wave is located at $u=u_0$. We consider an idealized scenario in which the spacetime is exactly Minkowski on either side of u_0.

The term $f(\vec{x})$ is the shock wave profile, which is directly related to the energy density $\varrho(\vec{x})$ through the Einstein field equations:

$$\Delta f(\vec{x})=-16\pi G_{\rm N}\varrho(\vec{x}), \qquad (34)$$

where $\Delta=\delta^{ij}\partial_i\partial_j$ is the flat Laplacian in the transverse direction. We use a quadratic profile given by

$$f(\vec{x}) = -\vec{x}\cdot A\cdot\vec{x} = -\sum_{i=1}^{D-2} a_i (x^i)^2, \tag{35}$$

where A is a symmetric constant matrix, whose eigenvalues are a_i. Such a profile represents an ultrarelativistic domain wall in the transverse plane [42],as one can see from (34) that the energy density is constant everywhere: $\varrho(\vec{x}) = \mathrm{Tr}[A]/8\pi G_\mathrm{N}$.

Using the notation $\mathsf{x} = (u, v, \vec{x})$ and $\mathsf{y} = (U, V, \vec{X})$ the exact form of the Wightman function is [20]

$$W(\mathsf{x},\mathsf{y}) = \frac{(-\mathrm{i})^{D-2}\Gamma(D/2-1)}{4\pi^{D/2}} \prod_{i=1}^{D-2}\left(1 + a_i\Delta\Theta\frac{(u-u_0-\mathrm{i}\epsilon)(U-u_0+\mathrm{i}\epsilon)}{\Delta u - \mathrm{i}\epsilon}\right)^{-1/2} \times\left((\Delta v-\mathrm{i}\epsilon)(\Delta u-\mathrm{i}\epsilon) - \Delta\vec{x}^2 + \sum_{i=1}^{D-2}\frac{a_i\Delta\Theta([U-u_0+\mathrm{i}\epsilon]x^i - [u-u_0-\mathrm{i}\epsilon]X^i)^2}{\Delta u - \mathrm{i}\epsilon + a_i\Delta\Theta(u-u_0-\mathrm{i}\epsilon)(U-u_0+\mathrm{i}\epsilon)}\right)^{(2-D)/2}, \tag{36}$$

where $\Delta v \equiv v - V$, $\Delta u \equiv u - U$, $\Theta_u \equiv \Theta(u-u_0)$, and $\Delta\Theta = \Theta_u - \Theta_U$ with the Heaviside step function $\Theta(u)$. $\Gamma(x)$ is the gamma function and by choosing $D = 4$ it gives $\Gamma(1) = 1$. The Wightman function reduces to the standard Minkowski space form if $f(\vec{x}) = 0$ (in which case there is no shock wave at all) or $\Delta\Theta = 0$ (so the events u and U are localized at the same side of the shock wave).

B. Results

We restrict to $D = 4$ and consider two inertial UDW detectors:

$$\mathsf{x}_\mathrm{A}(\tau_\mathrm{A}) = (t(\tau_\mathrm{A}), x(\tau_\mathrm{A}), y(\tau_\mathrm{A}), z(\tau_\mathrm{A})) = (\tau_\mathrm{A}, 0, 0, z_\mathrm{A}),$$
$$\mathsf{x}_\mathrm{B}(\tau_\mathrm{B}) = (t(\tau_\mathrm{B}), x(\tau_\mathrm{B}), y(\tau_\mathrm{B}), z(\tau_\mathrm{B})) = (\tau_\mathrm{B}, 0, 0, z_\mathrm{B}). \tag{37}$$

We further assume that $a_x = a_y \equiv a(>0)$ and $u_0 = 0$ as in Fig. 4 and $\vec{x} = \vec{X} = \vec{0}$. The Wightman function then reduces to

$$W(\mathsf{x},\mathsf{y}) = -\frac{1}{4\pi^2}\frac{1}{1 + a\Delta\Theta\frac{(u-\mathrm{i}\epsilon)(U+\mathrm{i}\epsilon)}{\Delta u - \mathrm{i}\epsilon}}\frac{1}{(\Delta v - \mathrm{i}\epsilon)(\Delta u - \mathrm{i}\epsilon)}. \tag{38}$$

It is worth noting that in this setup, the proper spatial distance between the two detectors, $L = |z_\mathrm{A} - z_\mathrm{B}|$, is the same as in Minkowski space, and that the two detectors are placed in the longitudinal direction of the shock wave.

In Fig. 5(a), we plot the initial ($\mathcal{C}_{\mathrm{AB},0}$) and final ($\mathcal{C}_\mathrm{AB}$) concurrences in the shock wave spacetime with $aT = 1$. In all figures, detector B is fixed at the position $z_\mathrm{B}/T = 7$ which is located on the $u < u_0$ part of shock wave spacetime (see Fig. 4) and the energy gap is $\Omega T = 2$. Note that in Minkowski space, the noncommunicating detectors cannot extract entanglement with $\Omega T = 2$, as shown in Figs. 2(a) and 3.

Figure 5(a–i) depicts the concurrences as functions of detector A's static positions z_A/T when $\beta = 10^{-5}$. As shown in Fig. 4, detector A encounters the shock wave around $z_\mathrm{A}/T = 0$. For $z_\mathrm{A}/T \lesssim -1$ the plot indicates that full entanglement degradation from the initial value of $\mathcal{C}_{\mathrm{AB},0}$ occurs, due to the fact that the geometry is Minkowski except along the shock wave trajectory. In other words, the behavior in $z_\mathrm{A}/T \lesssim -1$ follows from the results in Minkowski spacetime given in Figs. 2 and 3. This is also true for $z_\mathrm{A}/T \gtrsim 0.5$. The growth of $\mathcal{C}_\mathrm{AB}$ in $z_\mathrm{A}/T > 3$ comes from the communication effect in $|X_\mathrm{AB}(-\Omega)|$ between the two detectors, which corresponds to the bottom left corner in Fig. 1(b). The effect of the shock wave can be seen in the region $z_\mathrm{A}/T \in [-1, 0.5]$; not only is the degradation effect reduced, but we find $\mathcal{C}_\mathrm{AB} > \mathcal{C}_{\mathrm{AB},0}$—the initial entanglement is enhanced!. Somewhat surprisingly, the shock wave allows causally disconnected

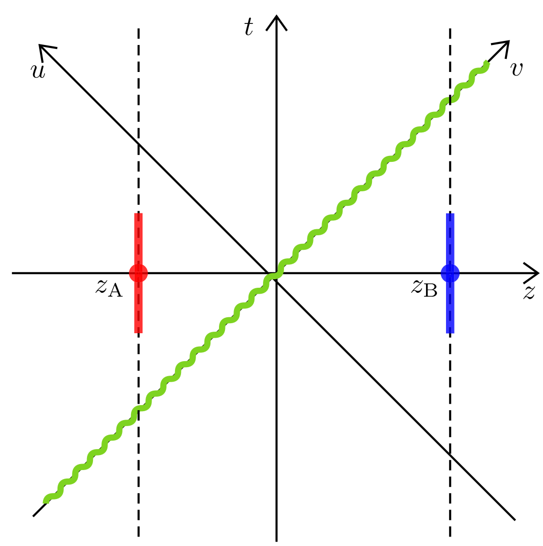

FIG. 4. Diagram for two pointlike inertial detectors in a shock wave spacetime. Detectors A and B are static at $z = z_\mathrm{A}$ and z_B, respectively, and the shock wave travels along $u = 0$ (the green wiggling line). The red and blue bars indicate the effective interaction duration of the detectors.

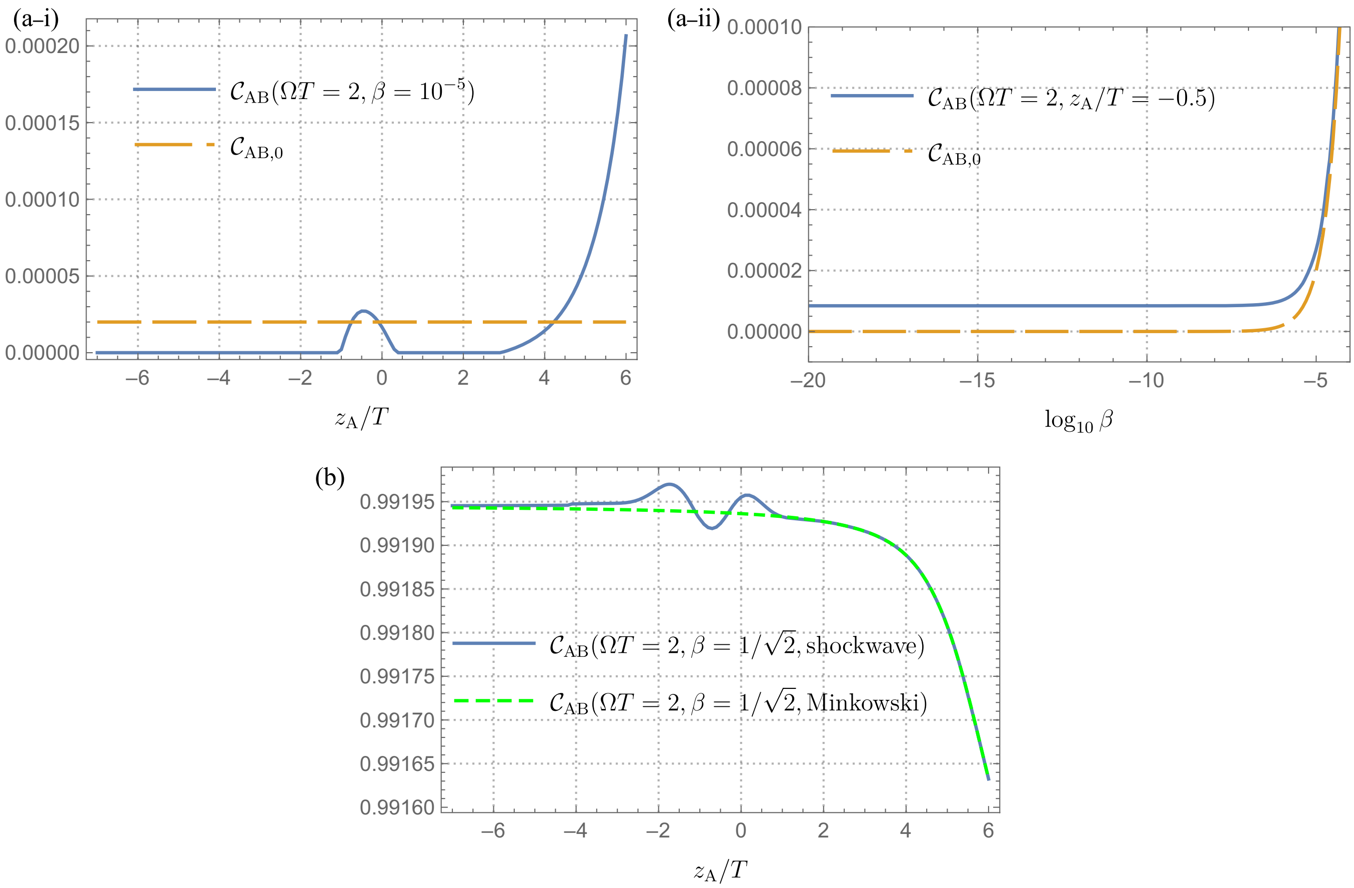

FIG. 5. (a–i) Initial and final concurrences when $\Omega T = 2$, $\beta = 10^{-5}$, $\lambda = 1/10$, and $\theta = 0$. The location of detector B is fixed at $z_{\rm B}/T = 7$. Detector A encounters the shock wave near $z_{\rm A}/T = 0$. (a–ii) The concurrences when $\Omega T = 2$, $z_{\rm A}/T = -0.5$ and $z_{\rm B}/T = 7$ with varying initial amount of entanglement. Two curves will cross and degradation takes place after $\log_{10}\beta > -3$. (b) Final concurrence $\mathcal{C}_{\rm AB}$ for initially maximally entangled detectors ($\mathcal{C}_{\rm AB,0} = 1$) with $\Omega T = 2$ and $\theta = 0$. The green dotted curve corresponds to detectors in Minkowski spacetime. In this case, the shock wave can either reduce or amplify the degradation effect.

detectors to gain more entanglement even when it is impossible to do this in Minkowski spacetime.

Figure 5(a–ii) shows the β dependence of the concurrences when $z_{\rm A}/T = -0.5$ (i.e., $L/T = 7.5$), where maximal entanglement enhancement occurs, with $\Omega T = 2$, $\lambda = 1/10$, and $\theta = 0$. We find that entanglement enhancement by the shock wave is possible so long as $\beta \lesssim 10^{-3}$. Recall that for any β, only degradation occurs for these parameters in Minkowski spacetime. Furthermore, even when $\Omega T = 7$ as in Figs. 2(b) and 2(c), the initial amount of entanglement needs to be $\beta \lesssim 10^{-17}$ in order to extract entanglement. In this sense, a shock wave drastically assists extraction of entanglement.

However, the shock wave does not always enhance entanglement. In Fig. 5(b), we plot the final concurrence when the detectors are initially maximally entangled, $\mathcal{C}_{\rm AB,0} = 1$. In both Minkowski (dotted curve) and shock wave (solid) spacetimes, degradation takes place as expected. Notice that the shock wave could either reduce or assist degradation. This is due to the fact that the concurrence is now determined by (28); the degradation part ${\rm Re}[Y_{\rm A} + Y_{\rm B}]$ is no longer suppressed by small β^2 and the harvesting part $|X_{\rm AB}(-\Omega)|$ is negligible.

V. CONCLUSION

We considered two initially entangled UDW detectors interacting with a quantum scalar field and examined how their initial entanglement behaves after the interaction. The entanglement harvesting protocol allows initially uncorrelated detectors to extract entanglement from the field in its vacuum state without signalling, whereas entanglement degradation is the process in which initial entanglement decreases due to the detectors becoming entangled with the field. We have investigated which phenomenon is dominant when the detectors are neither uncorrelated nor maximally entangled.

Such an analysis is known to be difficult when a perturbative method is employed since there is a UV-divergent element in the density matrix for the pointlike detectors (and hence in entanglement measures). One can circumvent this issue by introducing a smearing function and performing an approximation to an entanglement measure such as concurrence and negativity. We have dealt with this by introducing an approximation for weakly entangled detectors, supplementing the method used for initially sufficiently entangled detectors [35]. Under any of these approximations, the divergent element is absent in the entanglement measure.

With these approximations, we examined the fate of entanglement in detectors at rest in $(3+1)$-dimensional Minkowski spacetime. We found that *initially weakly entangled detectors can gain entanglement even when they are causally disconnected*. This can be understood by looking at the distinct contributions to the concurrence: one part is from the initial entanglement, another yields entanglement harvesting, and a third causes entanglement degradation. The detectors extract entanglement if the entanglement harvesting contribution to the concurrence exceeds the other two. Otherwise, entanglement degradation takes place and the initial amount of entanglement will be reduced after the interaction.

The fact that only weakly entangled detectors can gain entanglement is consistent with previous results (Ref. [34]) demonstrating that, nonperturbatively, quantum mutual information (i.e., total correlations including classical ones) between entangled detectors can be enhanced only when their initial entanglement is weak.[3] It is important to note, however, that the detectors can gain mutual information even when they are causally disconnected. Our results provide an interesting contrast insofar as we employ a perturbative analysis with a Gaussian switching function and near-pointlike detectors.

We have also analyzed the energy gap Ω dependence for entanglement extraction. In the entanglement harvesting scenario [12], detectors with Gaussian switching can extract entanglement so long as their energy gap is above the minimum value: $\Omega \geq \Omega_{\min}$. This feature allows one to harvest entanglement with detectors arbitrarily far away from each other once a sufficiently large energy gap is chosen. This is not the case for entangled detectors. Instead there is a range $\Omega \in [\Omega_{\min}, \Omega_{\max}]$ within which the detectors can extract entanglement. This range tends to zero as the distance between the detectors increases. This suggests that entanglement extraction is not allowed for detectors arbitrarily far away from each other. Nevertheless, the maximum value $\Omega_{\max}$ will increase as the initial state approaches a separable state, recovering the results of the standard entanglement harvesting protocol.

We found that the presence of a gravitational shock wave, in which the metric is identical to that of Minkowski spacetime except along a single null trajectory, significantly modifies these effects. Detectors far from the shock wave exhibit the same behavior as in Minkowski spacetime. However as they come closer to the shock wave their behavior markedly changes. The shock wave enhances entanglement as compared to Minkowski spacetime. The range $\Omega \in [\Omega_{\min}, \Omega_{\max}]$ of energy gap that enables entanglement extraction becomes wider, which in turn allows the detectors to gain entanglement for smaller values of Ω.

Although the shock wave enhances entanglement, its extraction is still limited to weakly entangled detectors. If the initial state of the detectors is sufficiently entangled, the shock wave weakens the effect of degradation rather than enhancing extraction of correlations. Nevertheless, our results show that spacetime geometry can enhance initial entanglement harvesting, indicating that the quantum vacuum is indeed a resource (at least in principle) for carrying out quantum information tasks.

We close by commenting on a recent similar investigation of the negativity [45] of two initially entangled detectors in Minkowski spacetime with constant switching. Using an approximation corresponding to our sufficiently entangled case, the detectors were found to only experience entanglement degradation, consistent with our results for sufficiently entangled detectors with an infinitely long interaction.

ACKNOWLEDGMENTS

This work was supported in part by the Natural Sciences and Engineering Research Council of Canada.

APPENDIX: SMEARED DETECTORS IN MINKOWSKI SPACETIME

The imaginary part of $\lambda^2 Y_k \equiv J_{kk}^{(-+)} + J_{kk}^{(+-)*}$ in r_{14} for pointlike detectors is known to be divergent. We will show that this term can be regularized by introducing finite-sized UDW detectors as suggested in [32]. In particular, we consider initially entangled smeared detectors at rest in $(3+1)$-dimensional Minkowski spacetime.

Assuming a massless scalar field, the mode decomposition of $\hat{\phi}(\mathsf{x}(t))$ is known to be

$$\hat{\phi}(t,\boldsymbol{x}) = \int \frac{\mathrm{d}^3 k}{\sqrt{(2\pi)^3 2|\boldsymbol{k}|}} (\hat{a}_{\boldsymbol{k}} e^{-\mathrm{i}|\boldsymbol{k}|t + \mathrm{i}\boldsymbol{k}\cdot\boldsymbol{x}} + \hat{a}_{\boldsymbol{k}}^\dagger e^{\mathrm{i}|\boldsymbol{k}|t - \mathrm{i}\boldsymbol{k}\cdot\boldsymbol{x}}), \quad \text{(A1)}$$

and so the Wightman function becomes

$$W(\mathsf{x}_j(t_1), \mathsf{y}_k(t_2)) = \int \frac{\mathrm{d}^3 k}{(2\pi)^3 2|\boldsymbol{k}|} e^{-\mathrm{i}|\boldsymbol{k}|(t_1 - t_2) + \mathrm{i}\boldsymbol{k}\cdot(\boldsymbol{x}-\boldsymbol{y})}. \quad \text{(A2)}$$

Let us first consider $\lambda^2 Y_{\mathrm{A}} \equiv J_{\mathrm{AA}}^{(-+)} + J_{\mathrm{AA}}^{(+-)*}$ for detector A in r_{14}. We find

[3] The nonperturbative method employed in [34] uses a delta-switching function, which cannot harvest entanglement at all if each detector switches only once [43,44].

$$J_{\rm AA}^{(-+)}+J_{\rm AA}^{(+-)*}$$
$$=-2\lambda_{\rm A}^2\int_{\mathbb{R}}\mathrm{d}t_1\int_{-\infty}^{t_1}\mathrm{d}t_2\chi_{\rm A}(t_1)\chi_{\rm A}(t_2)e^{-\mathrm{i}\Omega_{\rm A}(t_1-t_2)}\int\mathrm{d}^3xF_{\rm A}(\boldsymbol{x}-\boldsymbol{x}_{\rm A})\int\mathrm{d}^3yF_{\rm A}(\boldsymbol{y}-\boldsymbol{x}_{\rm A})\mathrm{Re}[W(\mathsf{x}_{\rm A}(t_1),\mathsf{y}_{\rm A}(t_2))] \tag{A3}$$
$$=-2\lambda_{\rm A}^2\int\frac{\mathrm{d}^3k}{2|\boldsymbol{k}|}\tilde{F}_{\rm A}(\boldsymbol{k})\tilde{F}_{\rm A}(-\boldsymbol{k})\int_{\mathbb{R}}\mathrm{d}t_1\int_{-\infty}^{t_1}\mathrm{d}t_2\chi_{\rm A}(t_1)\chi_{\rm A}(t_2)e^{-\mathrm{i}\Omega_{\rm A}(t_1-t_2)}\cos[|\boldsymbol{k}|(t_1-t_2)], \tag{A4}$$

where we have performed the Fourier transform:

$$\tilde{F}_j(\boldsymbol{k})=\int\frac{\mathrm{d}^3x}{\sqrt{(2\pi)^3}}F_j(\boldsymbol{x})e^{\mathrm{i}\boldsymbol{k}\cdot\boldsymbol{x}}. \tag{A5}$$

Note that $\tilde{F}_j(-\boldsymbol{k})=\tilde{F}_j(\boldsymbol{k})$ if $F_j(\boldsymbol{x})\in\mathbb{R}$. With a Gaussian switching centered at $t=t_{\rm A,0}$, $\chi_{\rm A}(t)=e^{-(t-t_{\rm A,0})^2/T^2}$,

$$\int_{\mathbb{R}}\mathrm{d}t_1\int_{-\infty}^{t_1}\mathrm{d}t_2e^{-(t_1-t_{\rm A,0})^2/T^2}e^{-(t_2-t_{\rm A,0})^2/T^2}e^{-\mathrm{i}\Omega_{\rm A}(t_1-t_2)}\cos[|\boldsymbol{k}|(t_1-t_2)]$$
$$=\frac{T\sqrt{2\pi}}{2}\int_0^\infty\mathrm{d}u\,e^{-u^2/2T^2}e^{-\mathrm{i}\Omega u}\cos(|\boldsymbol{k}|u) \tag{A6}$$
$$=\frac{\pi T^2}{4}e^{-T^2(|\boldsymbol{k}|+\Omega)^2/2}\left[1+e^{2|\boldsymbol{k}|T^2\Omega}\left(1+\mathrm{ierfi}\frac{T(|\boldsymbol{k}|-\Omega)}{\sqrt{2}}\right)-\mathrm{ierfi}\frac{T(|\boldsymbol{k}|+\Omega)}{\sqrt{2}}\right], \tag{A7}$$

and therefore, using the smearing function (30) and its Fourier transform, $\tilde{F}_j(\boldsymbol{k})=e^{-|\boldsymbol{k}|^2\sigma^2/4}/\sqrt{(2\pi)^3}$,

$$J_{\rm AA}^{(-+)}+J_{\rm AA}^{(+-)*}$$
$$=-\frac{\lambda_{\rm A}^2\pi T^2}{2}\int\frac{\mathrm{d}^3k}{2|\boldsymbol{k}|}\tilde{F}_{\rm A}^2(\boldsymbol{k})e^{-T^2(|\boldsymbol{k}|+\Omega)^2/2}\left[1+e^{2|\boldsymbol{k}|T^2\Omega}\left(1+\mathrm{ierfi}\frac{T(|\boldsymbol{k}|-\Omega)}{\sqrt{2}}\right)-\mathrm{ierfi}\frac{T(|\boldsymbol{k}|+\Omega)}{\sqrt{2}}\right] \tag{A8}$$
$$=-\frac{\lambda_{\rm A}^2e^{-T^2\Omega^2/2}}{8\pi(1+\sigma^2/T^2)^{3/2}}\left[2\sqrt{1+\sigma^2/T^2}+e^{T^2\Omega^2/2(1+\sigma^2/T^2)}\sqrt{2\pi}T\Omega\mathrm{erf}\frac{T\Omega}{\sqrt{2(1+\sigma^2/T^2)}}\right]$$
$$-\mathrm{i}\frac{\lambda_{\rm A}^2T^2}{8\pi}\int_0^\infty\mathrm{d}|\boldsymbol{k}||\boldsymbol{k}|e^{-|\boldsymbol{k}|^2\sigma^2/2}\left[e^{-T^2(|\boldsymbol{k}|-\Omega)^2/2}\mathrm{erfi}\frac{T(|\boldsymbol{k}|-\Omega)}{\sqrt{2}}-e^{-T^2(|\boldsymbol{k}|+\Omega)^2/2}\mathrm{erfi}\frac{T(|\boldsymbol{k}|+\Omega)}{\sqrt{2}}\right], \tag{A9}$$

where we have used $\mathrm{d}^3k=|\boldsymbol{k}|^2\sin\theta\mathrm{d}|\boldsymbol{k}|\mathrm{d}\theta\mathrm{d}\varphi$ with $|\boldsymbol{k}|\in[0,\infty)$, $\theta\in[0,\pi]$, and $\varphi\in[0,2\pi)$. The real and imaginary parts of $J_{kk}^{(-+)}+J_{kk}^{(+-)*}$ for smeared detectors are shown in Fig. 6.

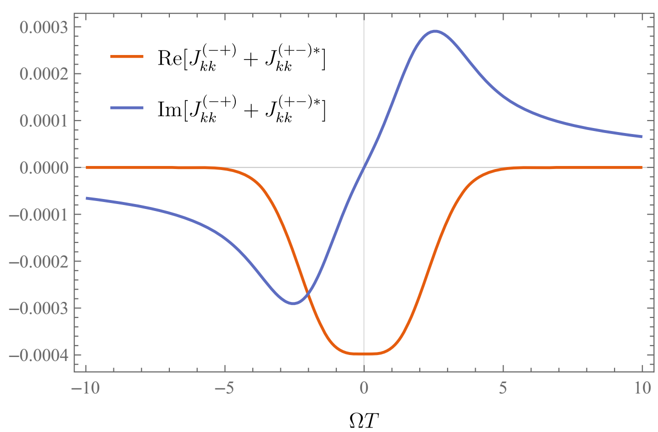

FIG. 6. Real and imaginary parts of $J_{kk}^{(-+)}+J_{kk}^{(+-)*}$ with $\sigma/T=1$ and $\lambda=1/10$. The real part converges quickly to 0 with large $|\Omega T|$ while the imaginary part is nonzero for a wide range of ΩT.

Similar calculations yield the remaining terms in r_{14}, r_{22}, and r_{33}. In particular, the expressions for $I_{kk}^{(-+)}$ in r_{22} and r_{33} in (31c) and for $J_{\mathrm{AB}}^{(++)}$ (and its counterparts) in (31b) that contribute to $\lambda^2 X_{\mathrm{AB}}^*(-\Omega) \equiv J_{\mathrm{AB}}^{(++)*} + J_{\mathrm{BA}}^{(++)*}$ in r_{14} can be found in Ref. [12].

[1] S. J. Summers and R. Werner, The vacuum violates Bell's inequalities, Phys. Lett. **110A**, 257 (1985).
[2] S. J. Summers and R. Werner, Bell's inequalities and quantum field theory. I. General setting, J. Math. Phys. (N.Y.) **28**, 2440 (1987).
[3] W. G. Unruh, Notes on black-hole evaporation, Phys. Rev. D **14**, 870 (1976).
[4] B. S. DeWitt, Quantum gravity: The new synthesis, in *General Relativity: An Einstein Centenary Survey*, edited by S. W. Hawking and W. Israel (Cambridge University Press, Cambridge, England, 1979), pp. 680–745.
[5] E. Martín-Martínez, M. Montero, and M. del Rey, Wave packet detection with the Unruh-Dewitt model, Phys. Rev. D **87**, 064038 (2013).
[6] A. M. Alhambra, A. Kempf, and E. Martín-Martínez, Casimir forces on atoms in optical cavities, Phys. Rev. A **89**, 033835 (2014).
[7] A. Pozas-Kerstjens and E. Martín-Martínez, Entanglement harvesting from the electromagnetic vacuum with hydrogenlike atoms, Phys. Rev. D **94**, 064074 (2016).
[8] A. Valentini, Non-local correlations in quantum electrodynamics, Phys. Lett. **153A**, 321 (1991).
[9] B. Reznik, Entanglement from the vacuum, Found. Phys. **33**, 167 (2003).
[10] B. Reznik, A. Retzker, and J. Silman, Violating Bell's inequalities in vacuum, Phys. Rev. A **71**, 042104 (2005).
[11] G. V. Steeg and N. C. Menicucci, Entangling power of an expanding universe, Phys. Rev. D **79**, 044027 (2009).
[12] A. Pozas-Kerstjens and E. Martín-Martínez, Harvesting correlations from the quantum vacuum, Phys. Rev. D **92**, 064042 (2015).
[13] H. Maeso-García, J. Polo-Gómez, and E. Martín-Martínez, Entanglement harvesting: State dependence and covariance, Phys. Rev. D **106**, 105001 (2022).
[14] E. Martín-Martínez, A. R. H. Smith, and D. R. Terno, Spacetime structure and vacuum entanglement, Phys. Rev. D **93**, 044001 (2016).
[15] S. Kukita and Y. Nambu, Harvesting large scale entanglement in de Sitter space with multiple detectors, Entropy **19**, 449 (2017).
[16] L. J. Henderson, R. A. Hennigar, R. B. Mann, A. R. H. Smith, and J. Zhang, Harvesting entanglement from the black hole vacuum, Classical Quantum Gravity **35**, 21LT02 (2018).
[17] K. K. Ng, R. B. Mann, and E. Martín-Martínez, Unruh-DeWitt detectors and entanglement: The anti–de Sitter space, Phys. Rev. D **98**, 125005 (2018).
[18] L. J. Henderson, R. A. Hennigar, R. B. Mann, A. R. Smith, and J. Zhang, Entangling detectors in anti-de Sitter space, J. High Energy Phys. 05 (**2019**) 178.
[19] W. Cong, C. Qian, M. R. Good, and R. B. Mann, Effects of horizons on entanglement harvesting, J. High Energy Phys. 10 (2020) 067.
[20] F. Gray, D. Kubizňák, T. May, S. Timmerman, and E. Tjoa, Quantum imprints of gravitational shockwaves, J. High Energy Phys. 11 (2021) 054.
[21] Z. Liu, J. Zhang, R. B. Mann, and H. Yu, Does acceleration assist entanglement harvesting?, Phys. Rev. D **105**, 085012 (2022).
[22] C. Suryaatmadja, R. B. Mann, and W. Cong, Entanglement harvesting of inertially moving Unruh-Dewitt detectors in Minkowski spacetime, Phys. Rev. D **106**, 076002 (2022).
[23] P. M. Alsing and G. J. Milburn, Teleportation with a Uniformly Accelerated Partner, Phys. Rev. Lett. **91**, 180404 (2003).
[24] I. Fuentes-Schuller and R. B. Mann, Alice Falls into a Black Hole: Entanglement in Noninertial Frames, Phys. Rev. Lett. **95**, 120404 (2005).
[25] P. M. Alsing, I. Fuentes-Schuller, R. B. Mann, and T. E. Tessier, Entanglement of Dirac fields in noninertial frames, Phys. Rev. A **74**, 032326 (2006).
[26] S.-Y. Lin, C.-H. Chou, and B. L. Hu, Disentanglement of two harmonic oscillators in relativistic motion, Phys. Rev. D **78**, 125025 (2008).
[27] S.-Y. Lin and B. L. Hu, Temporal and spatial dependence of quantum entanglement from a field theory perspective, Phys. Rev. D **79**, 085020 (2009).
[28] A. G. S. Landulfo and G. E. A. Matsas, Sudden death of entanglement and teleportation fidelity loss via the Unruh effect, Phys. Rev. A **80**, 032315 (2009).
[29] J. Doukas and B. Carson, Entanglement of two qubits in a relativistic orbit, Phys. Rev. A **81**, 062320 (2010).
[30] L. C. Céleri, A. G. S. Landulfo, R. M. Serra, and G. E. A. Matsas, Sudden change in quantum and classical correlations and the Unruh effect, Phys. Rev. A **81**, 062130 (2010).
[31] D. C. M. Ostapchuk, S.-Y. Lin, R. B. Mann, and B. L. Hu, Entanglement dynamics between inertial and non-uniformly accelerated detectors, J. High Energy Phys. 07 (2012) 072.
[32] E. Martín-Martínez and J. Louko, $(1+1)$D Calculation Provides Evidence that Quantum Entanglement Survives a Firewall, Phys. Rev. Lett. **115**, 031301 (2015).
[33] C. Rodríguez-Camargo, G. Menezes, and N. Svaiter, Finite-time response function of uniformly accelerated entangled atoms, Ann. Phys. (Amsterdam) **396**, 266 (2018).
[34] K. Gallock-Yoshimura and R. B. Mann, Entangled detectors nonperturbatively harvest mutual information, Phys. Rev. D **104**, 125017 (2021).
[35] P. Chowdhury and B. R. Majhi, Fate of entanglement between two Unruh-DeWitt detectors due to their motion

and background temperature, J. High Energy Phys. 05 (2022) 025.

[36] M. S. Soares, N. F. Svaiter, and G. Menezes, Entanglement dynamics: Generalized master equation for uniformly accelerated two-level systems, Phys. Rev. A **106**, 062440 (2022).

[37] E. Tjoa and E. Martín-Martínez, When entanglement harvesting is not really harvesting, Phys. Rev. D **104**, 125005 (2021).

[38] M. Cliche and A. Kempf, Vacuum entanglement enhancement by a weak gravitational field, Phys. Rev. D **83**, 045019 (2011).

[39] T. Dray and G. 't Hooft, The gravitational shock wave of a massless particle, Nucl. Phys. **B253**, 173 (1985).

[40] P. C. Aichelburg and R. U. Sexl, On the gravitational field of a massless particle, Gen. Relativ. Gravit. **2**, 303 (1971).

[41] H. Brinkmann, On Riemann spaces conformal to Euclidean space, Proc. Natl. Acad. Sci. U.S.A. **9**, 1 (1923).

[42] C. Loustó and N. Sánchez, Gravitational shock waves generated by extended sources: Ultrarelativistic cosmic strings, monopoles and domain walls, Nucl. Phys. **B355**, 231 (1991).

[43] P. Simidzija and E. Martín-Martínez, Nonperturbative analysis of entanglement harvesting from coherent field states, Phys. Rev. D **96**, 065008 (2017).

[44] P. Simidzija, R. H. Jonsson, and E. Martín-Martínez, General no-go theorem for entanglement extraction, Phys. Rev. D **97**, 125002 (2018).

[45] D. Barman, A. Choudhury, B. Kad, and B. R. Majhi, Spontaneous entanglement leakage of two static entangled Unruh-Dewitt detectors, Phys. Rev. D **107**, 045001 (2023).